Si xiii Emission Lines in Solar Flare X-ray Spectra Obtained with the *P78-1* Satellite
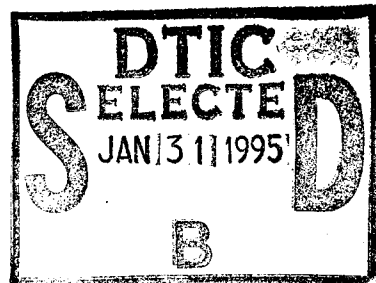
1 November 1994

Prepared by

F. P. KEENAN and E. S. CONLON
The Queen's University of Belfast
Northern Ireland, UK

D. L. McKENZIE
Space and Environment Technology Center
Technology Operations
The Aerospace Corporation

and

K. J. H. PHILLIPS
Rutherford Appleton Laboratory
England, UK

DTIC
ELECTE
JAN 31 1995
B

DTIC QUALITY INSPECTED 5

THE AEROSPACE
CORPORATION
El Segundo, California

1995 0125 002

LESLIE BELSMA, MAJ, USAF
MOIE Project Officer

NATHAN A. KIRBY
Deputy, Industrial and International Division
Plans and Programs Directorate
Phillips Laboratory

Accession For

NTIS GRA&I	☑	
DTIC TAB	☐	
Unannounced	☐	
Justification		

By
Distribution/
Availability Codes
Avail and/or
Dist Special

A-1

REPORT DOCUMENTATION PAGE

Form Approved
OMB No. 0704-0188

1. AGENCY USE ONLY (*Leave blank*)	2. REPORT DATE	3. REPORT TYPE AND DATES COVERED

4. TITLE AND SUBTITLE

Si XIII Emission Lines in Solar Flare X-ray Spectra Obtained with the *P78-1* Satellite

6. AUTHOR(S) Keenan, F. P., and Conlon, E. S. (University of Belfast); McKenzie, D. L. (The Aerospace Corporation); and Phillips, K. J. H. (Rutherford Appleton Laboratory)

5. FUNDING NUMBERS

F04701-88-C-0089

7. PERFORMING ORGANIZATION NAME(S) AND ADDRESS(ES)

The Aerospace Corporation
Technology Operations
El Segundo, CA 90245-4691

8. PERFORMING ORGANIZATION REPORT NUMBER

TR-93(3940)-14

9. SPONSORING/MONITORING AGENCY NAME(S) AND ADDRESS(ES)

Space and Missile Systems Center
Air Force Materiel Command
2430 E. El Segundo Blvd.
Los Angeles Air Force Base, CA 90245

10. SPONSORING/MONITORING AGENCY REPORT NUMBER

SMC-TR-94-47

11. SUPPLEMENTARY NOTES

12a. DISTRIBUTION/AVAILABILITY STATEMENT

Approved for public release; distribution unlimited

12b. DISTRIBUTION CODE

13. ABSTRACT (*Maximum 200 words*)

Theoretical Si XIII electron-temperature–sensitive emission-line ratios, which include satellite-line contributions to the intensities of the forbidden *(f)* $1s^2 \, {}^1S–1s2s \, {}^3S$, intercombination *(i)* $1s^2 \, {}^1S–1s2p \, {}^3P_{1,2}$, and resonance *(r)* $1s^2 \, {}^1S–1s2p \, {}^1P$ transitions, are presented for $G = [I(f) + I(i)]/I(r)$, $R = I(f)/I(i)$, $R_1 = I(1s^2 \, {}^1S–1s3p \, {}^1P)/I(r)$, and $R_2 = I(1s^2 \, {}^1S–1s4p \, {}^1P)/I(r)$. These ratios are significantly different from those calculated assuming that satellites do not contribute to f, i, and r, and, in addition, are more temperature-sensitive over the range $\log T_e = 6.4$–7.4. Electron temperatures deduced using the new diagnostics in conjunction with observed values of G, R_1, and R_2 from solar-flare spectra obtained by the SOLEX spectrometers aboard the P78-1 satellite are found to be generally consistent. This provides support for the validity of the theoretical R_1 and R_2 diagnostics and also resolves discrepancies noted previously when the line ratios were compared with observations from the *Solar Maximum Mission* spectrometers. The R ratio, which is in the low-density limit under solar flare conditions, is found not to be a useful T_e diagnostic when satellite contributions to f and i are included in the theoretical line ratios. However, the observed values of R from the SOLEX spectra are in good agreement with theoretical predictions, which provides additional support for the accuracy of the line-ratio calculations.

14. SUBJECT TERMS
Atomic Data
Solar Flares
Solar X-rays

15. NUMBER OF PAGES
9

16. PRICE CODE

17. SECURITY CLASSIFICATION OF REPORT	18. SECURITY CLASSIFICATION OF THIS PAGE	19. SECURITY CLASSIFICATION OF ABSTRACT	20. LIMITATION OF ABSTRACT
Unclassified	Unclassified	Unclassified	

Standard Form 298 (Rev. 2-89)
Prescribed by ANSI Std. Z39-18
298-102

Si XIII EMISSION LINES IN SOLAR FLARE X-RAY SPECTRA OBTAINED WITH THE *P78-1* SATELLITE

F. P. Keenan,[1] D. L. McKenzie,[2] K. J. H. Phillips,[3] AND E. S. Conlon[1]

ABSTRACT

Theoretical Si XIII electron-temperature–sensitive emission-line ratios, which include satellite-line contributions to the intensities of the forbidden (f) $1s^2\ {}^1S$–$1s2s\ {}^3S$, intercombination (i) $1s^2\ {}^1S$–$1s2p\ {}^3P_{1,2}$, and resonance (r) $1s^2\ {}^1S$–$1s2p\ {}^1P$ transitions, are presented for $G = [I(f) + I(i)]/I(r)$, $R = I(f)/I(i)$, $R_1 = I(1s^2\ {}^1S$–$1s3p\ {}^1P)/I(r)$, and $R_2 = I(1s^2\ {}^1S$–$1s4p\ {}^1P)/I(r)$. These ratios are significantly different from those calculated assuming that satellites do not contribute to f, i, and r, and, in addition, are more temperature-sensitive over the range log $T_e = 6.4$–7.4. Electron temperatures deduced using the new diagnostics in conjunction with observed values of G, R_1, and R_2 from solar-flare spectra obtained by the SOLEX spectrometers aboard the *P78-1* satellite are found to be generally consistent. This provides support for the validity of the theoretical R_1 and R_2 diagnostics and also resolves discrepancies noted previously when the line ratios were compared with observations from the *Solar Maximum Mission* spectrometers. The R ratio, which is in the low-density limit under solar flare conditions, is found not to be a useful T_e diagnostic when satellite contributions to f and i are included in the theoretical line ratios. However, the observed values of R from the SOLEX spectra are in good agreement with theoretical predictions, which provides additional support for the accuracy of the line-ratio calculations.

Subject headings: atomic data — Sun: flares — Sun: X-rays, gamma rays

1. INTRODUCTION

The three principal lines of ions in the He I isoelectronic series, namely, the forbidden (f) $1s^2\ {}^1S$–$1s2s\ {}^3S$, intercombination (i) $1s^2\ {}^1S$–$1s2p\ {}^3P_{1,2}$, and resonance (r) $1s^2\ {}^1S$–$1s2p\ {}^1P$ transitions, are frequently observed in solar X-ray spectra (see, for example, Phillips et al. 1982; Doschek 1990). They may be used to infer the electron temperature T_e and density N_e of the emitting plasma through the well-known line intensity ratios $G = [I(f) + I(i)]/I(r)$ and $R = I(f)/I(i)$, respectively (Gabriel & Jordan 1972; Bluementhal, Drake, & Tucker 1972). However, the theoretical values of these ratios are critically dependent on the atomic data adopted in their calculation, especially the electron-impact excitation rates between the $1s^2\ {}^1S$ ground state and the $1s2l$ levels (Gabriel & Jordan 1972). Over the last few years, there have been many theoretical determinations of G and R, with the most accurate currently available probably being those of Keenan and coworkers for ions between O VII and Ar XVII (Keenan, Tayal, & Kingston 1984; Keenan & McCann 1987; McCann & Keenan 1987, 1988; Keenan et al. 1987, 1989, 1991, 1992; Coffey et al. 1993; Phillips et al. 1994), which are based on electron excitation rates derived with the R-matrix code of Burke & Robb (1975).

Keenan, Kingston, & McKenzie (1985, 1986) and Keenan et al. (1987) have extended the above work to derive emission-line ratios in O VII, Ne IX, and Mg XI, involving the $1s^2\ {}^1S$–$1snp\ {}^1P$, $n = 2, 3$, and 4, transitions, namely, $R_1 = I(1s^2\ {}^1S$–$1s3p\ {}^1P)/I(r)$

and $R_2 = I(1s^2\ {}^1S$–$1s4p\ {}^1P)/I(r)$. These ratios are more sensitive to electron temperature than the G ratio, which is frequently used as a temperature diagnostic for the He I isoelectronic series. These authors compared their results with solar observations from the SOLEX spectrometers and found excellent agreement between electron temperatures deduced from G and from R_1 and R_2.

More recently, Keenan, McCann, & Phillips (1990) calculated R_1 and R_2 ratios for Si XIII. They found reasonable agreement between their results and observations from several spacecraft experiments, but notably not those from the Flat Crystal Spectrometer on the *Solar Maximum Mission* spacecraft, the discrepancy most likely being associated with the observations. In this paper, we extend the investigation of Keenan et al. (1990) by comparing the Si XIII theoretical ratios with solar spectra from the SOLEX scanning spectrometer on the *P78-1* satellite.

2. THEORETICAL RATIOS

The atomic data adopted in the line-ratio calculations have been summarized by Keenan et al. (1989). Briefly, the 23 $1snl$ states with $n < 6$ and $l < 3$ were included in the model ion, making a total of 37 levels when the fine-structure splitting in the triplet terms was included. The only atomic processes considered were collisional excitation and deexcitation by electrons, spontaneous radiative decay, and dielectronic and radiative recombination to the $n = 2$ levels, and the plasma was assumed to be optically thin and in coronal equilibrium. Further details may be found in Keenan et al. (1989).

Keenan et al. (1989, 1990) used the model ion discussed above to derive theoretical values of the following T_e-sensitive emission-line ratios: G, R_1, and R_2. However, as noted by, for example, Phillips et al. (1994), dielectronic-recombination satellites due to the lithium-like ion, with transitions $1s^2nl$–

[1] Department of Pure and Applied Physics, The Queen's University of Belfast, Belfast BT7, 1NN, Northern Ireland, UK.

[2] Space and Environment Technology Center, The Aerospace Corporation, M2-266, P.O. Box 92957, Los Angeles, CA 90009

[3] Astrophysics Division, Rutherford Appleton Laboratory, Chilton, Didcot, Oxfordshire OX11 0QX, England, UK.

$1s2pnl$ (nonparticipating or "spectator" electron having quantum numbers nl, $n \geq 2$) make an important contribution to the measured intensities of the f, i, and r lines for species with atomic numbers $Z \geq 12$. Thus, the two strong satellites j ($1s^22p$ $^2P_{3/2}$–$1s2p^2$ $^2D_{5/2}$) and k ($1s^22p$ $^2P_{1/2}$–$1s2p^2$ $^2D_{3/2}$) blend with the f line (Gabriel 1972), while numerous unresolved weak satellites converge on the r line from the long-wavelength side for increasing values of the principal quantum number n of the spectator electron (Summers 1973). In view of this, we have used the results of Vainshtein & Safronova (1978) to recalculate theoretical values of G, R, R_1, and R_2, which include the contributions of the strong satellite lines with wavelengths that lie within 10 mÅ of the f, i, and r lines. In Figures 1–3 these ratios are plotted as functions of the electron temperature for $N_e = 10^{11}$ cm^{-3}, although we note that G, R_1, and R_2 are insensitive to density for $N_e \leq 10^{14}$ cm^{-3}. Also shown in the figures are the theoretical ratios from Keenan et al. (1989, 1990), which exclude any satellite contributions to f, i, and r.

An inspection of Figures 1–3 reveals that theoretical ratios that include the satellite contributions are significantly different from those that do not, especially at low temperatures, which is expected, as the satellite-line intensities have an approximate T^{-1} dependence (Gabriel 1972). In the cases of R_1 and R_2, the inclusion of the satellites leads to a decrease in the ratios by $\sim 40\%$ at log $T_e = 6.4$, but only 3% at log $T_e = 7.4$. This implies that the electron-temperature sensitivity of R_1 and R_2 is increased, as the ratios that do not include satellite blending increase by factors of 3.0 (R_1) and 4.3 (R_2) between log $T_e = 6.4$ and 7.4, while the ratios that include these contributions change by factors of 4.8 and 7.0, respectively, over the same temperature interval. This effect is even more pronounced for G, where satellites lead to a 57% increase in the
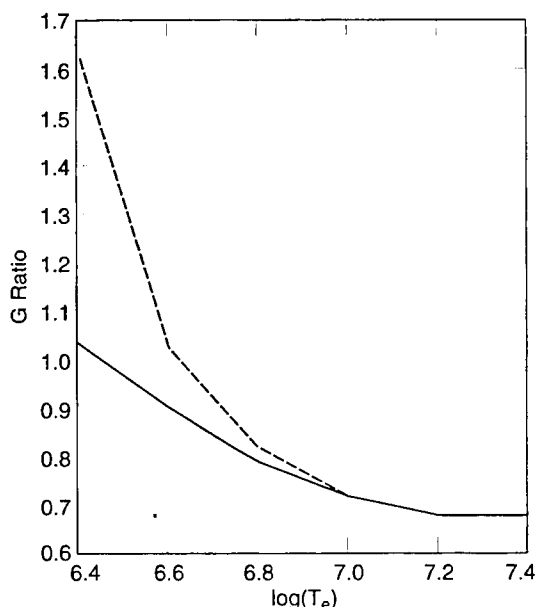

FIG. 2.—The theoretical Si XIII emission-line ratio $R_1 = I(1s^2$ ^1S–$1s3p$ $^1P)/I(r)$ plotted as a function of electron temperature at a density $N_e = 10^{11}$ cm^{-3}. The dashed line corresponds to calculations that include satellite-line contributions to $I(r)$, and the solid line corresponds to calculations excluding satellite lines.

FIG. 1.—The theoretical Si XIII emission-line ratio $G = [I(1s^2$ ^1S–$1s2s$ $^3S) + I(1s^2$ ^1S–$1s2p$ $^3P_{1,2})]/I(1s^2$ ^1S–$1s2p$ $^1P) \equiv [I(f) + I(i)]/I(r)$, where I is in units of photon numbers, plotted as a function of electron temperature at an electron density $N_e = 10^{11}$ cm^{-3}. The dashed-line curve is for calculations that include satellite-line contributions to the f, i, and r intensities, and the calculations corresponding to the solid-line curve exclude satellite lines.
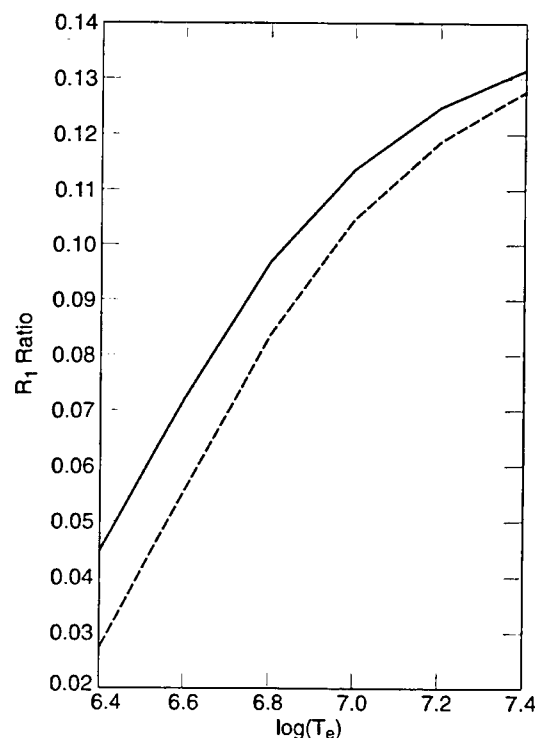

FIG. 3.—The theoretical Si XIII emission-line ratio $R_2 = I(1s^2$ ^1S–$1s4p$ $^1P)/I(r)$ plotted as a function of electron temperature at a density $N_e = 10^{11}$ cm^{-3}. The dashed line corresponds to calculations that include satellite-line contributions to $I(r)$, and the solid line corresponds to calculations excluding satellite lines.
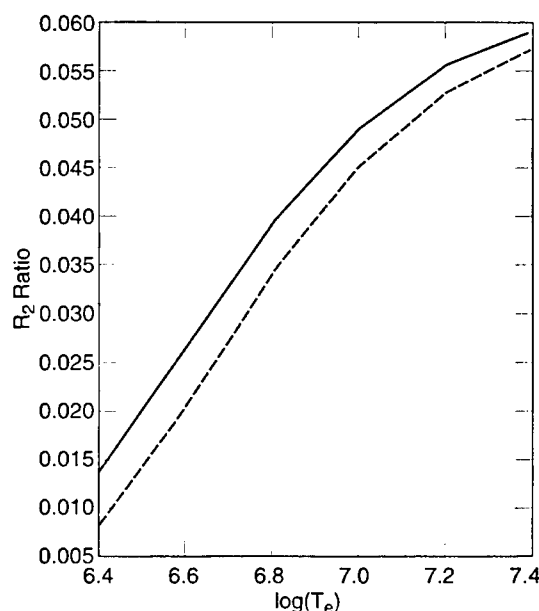
ratio at $\log T_e = 6.4$, but no change at $\log T_e = 7.4$. This implies an increase in the T_e sensitivity over the range $\log T_e = 6.4$–7.4 from a factor of 1.5 to a factor of 2.4.

3. OBSERVATIONAL DATA

The f, i, r, and $1s^2\ ^1S-1snp\ ^1P$, $n = 3$ and 4, emission lines in Si XIII have been observed at wavelengths of 6.738, 6.686, 6.646, 5.683, and 5.402 Å, respectively, in solar flare spectra obtained by the SOLEX A and SOLEX B ADP X-ray Bragg Crystal Spectrometers on the US Department of Defense *P78-1* satellite (McKenzie et al. 1985). In this paper, we consider only measurements made by the SOLEX A spectrometer, because the SOLEX B detector, a microchannel plate, has a discontinuity in its response at 6.75 Å, the wavelength of the Si K absorption edge (Eng & Landecker 1981). The instrument is described in McKenzie et al. (1980).

We have measured the intensities of the above lines in several solar flares using methods discussed in McKenzie & Landecker (1982). Unfortunately, in the SOLEX observations, the f line is blended with the Mg XII $1s\ ^2S-4p\ ^2P$ line, which also lies at 6.738 Å (Garcia & Mack 1965; Erickson 1977). We estimate the contribution of the Mg XII line to the apparent f line flux based on measurement of the Mg XII $1s\ ^2S-3p\ ^2P$ line at 7.107 Å (McKenzie et al. 1985); Garcia & Mack (1965) place the last-mentioned line at 7.106 Å. The Mg XII $1s-3p$ line is measured by the same spectrometer as are the Si XIII lines and lies sufficiently close in wavelength to the Si XIII f line that instrumental uncertainties are negligible. To make the correction, we compute the rates of collisional excitation of the $3p$ and $4p$ levels from the ground state and set them equal to the radiative deexcitation rates. The collisional excitation coefficient is (Gabriel & Jordan 1972)

$$C_{1n} = 8.65 \times 10^{-6}\ \frac{1}{\omega_1}\ \frac{1}{T_e^{1/2}}\ \overline{\Omega_{1n}}\ \exp\left(\frac{-E_{1n}}{kT_e}\right). \quad (1)$$

In equation (1), ω_1 is the statistical weight of the ground state, $\overline{\Omega_{1n}}$ is the collision strength, E_{1n} is the excitation energy, and T_e is the electron temperature. The collision strength is approximated as

$$\overline{\Omega_{1n}} \approx \frac{8\pi}{\sqrt{3}}\ \frac{f_{1n}}{E_0}\ \omega_1\ \bar{g}\ . \quad (2)$$

Assuming that the parameter $\bar{g}$ (Van Regemorter 1962) is the same for both lines,[4] the ratio of the photon intensities is

$$\frac{I_{1s-4p}}{I_{1s-3p}} = \frac{f_{14}\lambda_{14}b_{41}\ \exp\left[-(E_{14}-E_{13})/kT_e\right]}{f_{13}\lambda_{13}b_{31}}\ . \quad (3)$$

In equation (3), the oscillator strengths f and the branching ratios b are the H I values from Wiese, Smith, & Glennon (1966), the wavelengths λ are from Garcia & Mack (1965), and the temperature is assumed to be 7 MK. By applying equation (3), we found that the Mg XII line contributed 6.2%–15.4% of the flux to the blend at 6.738 Å, with the average contribution being 9.6%. This correction is small and has little effect on the measured G ratios, which are listed in Table 1, along with the R_1 ratios and the single observed value of the R_2 ratio, observed for the 1980 April 8 flare, the only event in which the Si XIII $1s^2\ ^1S-1s4p\ ^1P$ line was measurable. The statistical

---

[4] According to approximations by Mewe (1972), $\bar{g}(1s-4p)$ is ~8% larger than $\bar{g}(1s-3p)$ at a temperature of 7 MK. Use of these approximations would have resulted in an average decrease in the Si XIII f line strength of less than 1%.

TABLE 1
OBSERVED Si XIII EMISSION-LINE RATIOS

Date	UT	G	R_1	R_2
1979 Mar 31	17:00	0.83 ± 0.03	0.144 ± 0.035	...
1979 Mar 31	23:21	0.60 ± 0.02	0.080 ± 0.030	...
1979 Apr 3	04:20	0.75 ± 0.03	0.052 ± 0.035	...
1980 Apr 4	16:00	0.72 ± 0.04	0.194 ± 0.048	...
1980 Apr 8	03:24	0.68 ± 0.02	0.194 ± 0.022	0.041 ± 0.018
1980 May 21	21:50	0.71 ± 0.05	0.095 ± 0.045	...
1981 May 5	14:09	0.68 ± 0.01	0.094 ± 0.019	...

uncertainties in the ratios are also given in the table; they are typically 4% for G and 33% for R_1. In Figure 4, we show the spectrum of the 1979 March 31, 17:00 UT flare, to illustrate the quality of the observational data.

4. RESULTS AND DISCUSSION

In Table 2 we list the electron temperatures derived from the observed values of G, R_1, and R_2 by using the calculations in Figures 1–3 that include the contributions of satellite lines to f, i, and r line intensities. An inspection of the table reveals that the temperatures estimated from G and R_1 for the 1979 April 3, 1980 May 21, and 1981 May 5 flares are consistent, with differences of ≤ 0.3 dex. Similarly, for the 1980 April 8 event, the values of T_e deduced from G and R_2 differ only by 0.2 dex. The accuracy of the present calculations for G has already been established by Keenan et al. (1989) through a comparison with tokamak plasma observations for which the temperature and density have been independently determined. Hence the above results provide support for the validity of the theoretical R_1 and R_2 diagnostics. More important, they also resolve the large discrepancies found when the theoretical ratios were compared with observations made with the Flat Crystal Spectrometer (FCS) on the *Solar Maximum Mission satellite*
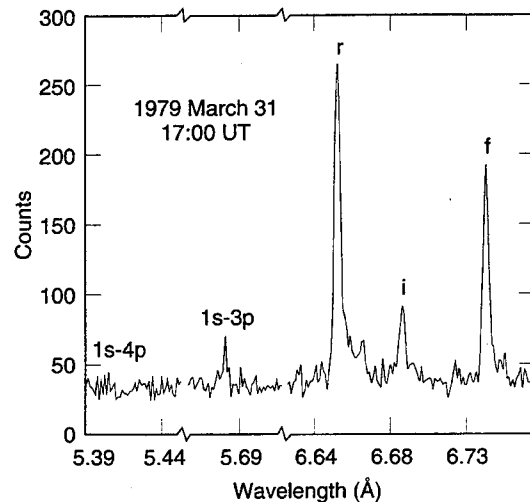

FIG. 4.—The Si XIII spectrum for the flare of 1979 March 31 at 17:00 UT, showing the r, i, f, and $1s^2\ ^1S-1s3p\ ^1P$, and $1s^2\ ^1S-1s4p\ ^1P$ lines. The last-mentioned line was not detected with sufficient statistical significance to allow it to be used in this study. Notice the breaks in the wavelength scale on the abscissa.

TABLE 2

log T_e Derived from Si xiii Line Ratios

Date	UT	G	R_1	R_2
1979 Mar 31	17:00	6.8	a	...
1979 Mar 31	23:21	b	6.8	...
1979 Apr 3	04:20	6.9	6.6	...
1980 Apr 4	16:00	7.0	a	...
1980 Apr 8	03:24	7.2	a	7.0
1980 May 21	21:50	7.0	6.9	...
1981 May 5	14:09	7.2	6.9	...

a Observed line ratio is larger than theoretical high-temperature limit.

b Observed line ratio is smaller than theoretical high-temperature limit.

TABLE 3

Observed and Theoretical Values of the R_0 Ratio for Si xiii

Date	UT	R (Observed)	log T_e	R_0 (Theory)
1979 Mar 31	17:00	2.62 ± 0.18	6.8	2.60
1979 Mar 31	23:21	2.99 ± 0.23	6.8	2.60
1979 Apr 3	0.4:20	2.74 ± 0.21	6.8	2.60
1980 Apr 4	16:00	3.02 ± 0.30	7.0	2.56
1980 Apr 8	03:24	2.79 ± 0.15	7.1	2.64
1980 May 21	21:50	2.95 ± 0.37	7.0	2.56
1981 May 5	14:09	2.58 ± 0.09	7.1	2.64

(Keenan et al. 1990). These discrepancies are either associated with the instrument or are due to time variations of line fluxes within the spectral scan duration.

For the 1979 March 31 flare at 1700 UT and the 1980 April 4 and 8 events, the R_1 ratios are larger than the theoretical high-temperature limits (see Table 2), although reducing these ratios by their observational uncertainties (see § 3) would lead to electron temperature estimates compatible with those deduced from G. However, the G ratio for the 1979 March 31 flare at 2321 UT is 12% smaller than the theoretical high-temperature limit, which is well outside the observational error (§ 3). A possible explanation for this is that the flare is not in

FIG. 5.—The theoretical Si xiii emission-line ratio $R_0 = I(f)/I(i)$, plotted as a function of electron temperature at a density $N_e = 10^{11}$ cm^{-3}. The dashed line corresponds to calculations that include satellite-line contributions to $I(f)$ and $I(i)$, and the solid line corresponds to calculations excluding satellite lines.

ionization equilibrium, with the H-like ion number density being very low. Under these conditions, dielectronic and radiative recombination of H-like Si xiv would not be important mechansims for populating the $1s2s$ ^3S and $1s2p$ ^3P levels of Si xiii, leading to a decrease in the predicted value of G, but not R_1, as the latter is relatively insensitive to recombination processes (see Fig. 3 of McCann & Keenan 1987 and Fig. 1 of Keenan et al. 1990). (The correction for Mg xii blending of the f line in this flare was only 8.5% and so cannot account for the small measured G ratio.) It is interesting to note that the measured G ratio for the 1979 March 31, 2321 UT flare (G = 0.60) would imply log T_e = 6.8 in the absence of dielectronic and radiative recombination (McCann & Keenan 1987), in excellent agreement with the temperature estimated from R_1. On the other hand, it is difficult to understand why the plasma in this flare alone should be transiently ionizing; the observations were not made during the rapid rise phase of the flare. However, we can offer no other explanation for this apparent discrepancy between theory and observation.

Finally, we note that the $R = I(f)/I(i)$ ratio is predicted to be density sensitive under solar plasma conditions for the He-like ions C v, O vii, Ne ix, and Mg xi (McKenzie et al. 1980; Doyle 1980; McKenzie 1987; Linford & Wolfson 1988). The Si xiii R ratio is only density sensitive for $N_e \geq 10^{13}$ cm^{-3} (Keenan et al. 1989), and hence one would expect this ratio to be in its low-density limit (called R_0) in solar coronal plasmas. In Figure 5, we therefore plot R_0 as a function of temperature, where, as before, we have both included and excluded the contribution of satellites to the f and i line intensities. An inspection of the figure reveals that, as with G, R_1, and R_2, the inclusion of satellites leads to very large changes in the theoretical values of R_0, especially at low electron temperatures. In addition, R_0 no longer increases monotonically with T_e, but rather decreases rapidly up to log T_e = 7.0, and then increases slowly. This implies that R_0 cannot be used as an electron temperature diagnostic. Although it is not possible to estimate temperatures reliably from R_0, it is still useful to compare theoretical and observed values of the ratio. In Table 3 we summarize R_0 ratios measured from the SOLEX flare observations discussed in § 3; the statistical uncertainties are included in the table. Also listed in the table are the theoretical values of R_0, which have been derived using the flare electron temperatures in Table 2 in conjunction with the calculations illustrated in Figure 5 that include satellite contributions to i and f. An inspection of the table reveals excellent agreement between theory and observation, with discrepancies that average only 9%, which is within the typical observational uncertainty. This provides further support for the accuracy of the theoretical line ratios, and hence the atomic data used in their calculation.
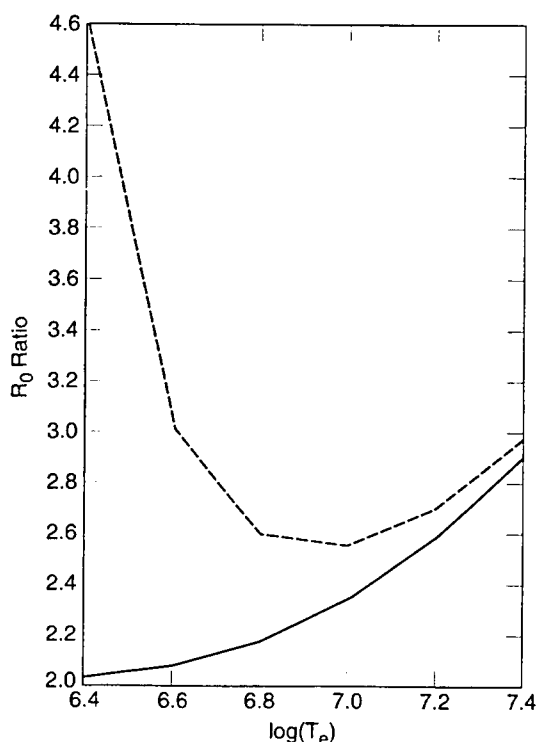
REFERENCES

Blumenthal, G. T., Drake, G. W. F., & Tucker, W. H. 1972, ApJ, 172, 205
Burke, P. G., & Robb, W. D. 1975, Adv. Atom. Molec. Phys., 11, 143
Coffey, I. H., Keenan, F. P., McAdam, C., Barnsley, R., Dickson, W. J., Lawson, K. D., & Peacock, N. J. 1993, Phys. Scripta, 47, 169
Doschek, G. A. 1990, ApJS, 73, 117
Doyle, J. G. 1980, A&A, 87, 183
Eng, W., & Landecker, P. B. 1981, Nucl. Inst. Meth., 190, 149
Erickson, G. W. 1977, J. Phys. Chem. Ref. Data, 6, 831
Gabriel, A. H. 1972, MNRAS, 160, 99
Gabriel, A. H., & Jordan, C. 1972, in Case Studies in Atomic Physics, Vol. 2, ed. E. W. McDaniel & M. R. C. McDowell (Amsterdam: North-Holland), 209
Garcia, J. D., & Mack, J. E. 1965, J. Opt. Soc. Am., 55, 654
Keenan, F. P., Kingston, A. E., & McKenzie, D. L. 1985, ApJ, 291, 855
————. 1986, ApJ, 303, 486
Keenan, F. P., & McCann, S. M. 1987, Sol. Phys., 109, 31
Keenan, F. P., McCann, S. M., Barnsley, R., Dunn, J., Evans, K. D., & Peacock, N. J. 1989, Phys. Rev. A, 39, 4092
Keenan, F. P., McCann, S. M., Kingston, A. E., Barnsley, R., Dunn, J., & Peacock, N. J. 1991, Phys. Rev. A, 44, 3831
Keenan, F. P., McCann, S. M., & Phillips, K. J. H. 1990, ApJ, 363, 310
Keenan, F. P., McKenzie, D. L., McCann, S. M., & Kingston, A. E. 1987, ApJ, 318, 926

Keenan, F. P., Phillips, K. J. H., Harra, L. K., Conlon, E. S., & Kingston, A. E. 1992, ApJ, 393, 815
Keenan, F. P., Tayal, S. S., & Kingston, A. E. 1984, Sol. Phys., 92, 75
Linford, G. A., & Wolfson, C. J. 1988, ApJ, 331, 1036
McCann, S. M., & Keenan, F. P. 1987, Sol. Phys., 112, 83
————. 1988, ApJ, 328, 344
McKenzie, D. L. 1987, ApJ, 322, 512
McKenzie, D. L., Broussard, R. M., Landecker, P. B., Rugge, H. R., Young, R. M., Doschek, G. A., & Feldman, U. 1980, ApJ, 238, L43
McKenzie, D. L., & Landecker, P. B. 1982, ApJ, 259, 372
McKenzie, D. L., Landecker, P. B., Broussard, R. M., Rugge, H. R., Young, R. M., Feldman, U., & Doschek, G. A. 1980, ApJ, 241, 409
McKenzie, D. L., Landecker, P. B., Feldman, U., & Doschek, G. A. 1985, ApJ, 289, 849
Mewe, R. 1972, A&A, 20, 215
Phillips, K. J. H., et al. 1982, ApJ, 256, 774
Phillips, K. J. H., Keenan, F. P., Harra, L. K., McCann, S. M., Rachlew-Kallne, E., Rice, J., & Wilson, M. 1994, J. Phys. B, submitted
Summers, H. P. 1973, ApJ, 179, L45
Vainshtein, L. A., & Safronova, U. I. 1978, Atom. Data Nucl. Data, 21, 49
Van Regemorter, H. 1962, ApJ, 136, 906
Wiese, W. L., Smith, M. W., & Glennon, B. M. 1966, Atomic Transition Probabilities (Washington: US GPO), 2

TECHNOLOGY OPERATIONS

The Aerospace Corporation functions as an "architect-engineer" for national security programs, specializing in advanced military space systems. The Corporation's Technology Operations supports the effective and timely development and operation of national security systems through scientific research and the application of advanced technology. Vital to the success of the Corporation is the technical staff's wide-ranging expertise and its ability to stay abreast of new technological developments and program support issues associated with rapidly evolving space systems. Contributing capabilities are provided by these individual Technology Centers:

Electronics Technology Center: Microelectronics, solid-state device physics, VLSI reliability, compound semiconductors, radiation hardening, data storage technologies, infrared detector devices and testing; electro-optics, quantum electronics, solid-state lasers, optical propagation and communications; cw and pulsed chemical laser development, optical resonators, beam control, atmospheric propagation, and laser effects and countermeasures; atomic frequency standards, applied laser spectroscopy, laser chemistry, laser optoelectronics, phase conjugation and coherent imaging, solar cell physics, battery electrochemistry, battery testing and evaluation.

Mechanics and Materials Technology Center: Evaluation and characterization of new materials: metals, alloys, ceramics, polymers and their composites, and new forms of carbon; development and analysis of thin films and deposition techniques; nondestructive evaluation, component failure analysis and reliability; fracture mechanics and stress corrosion; development and evaluation of hardened components; analysis and evaluation of materials at cryogenic and elevated temperatures; launch vehicle and reentry fluid mechanics, heat transfer and flight dynamics; chemical and electric propulsion; spacecraft structural mechanics, spacecraft survivability and vulnerability assessment; contamination, thermal and structural control; high temperature thermomechanics, gas kinetics and radiation; lubrication and surface phenomena.

Space and Environment Technology Center: Magnetospheric, auroral and cosmic ray physics, wave-particle interactions, magnetospheric plasma waves; atmospheric and ionospheric physics, density and composition of the upper atmosphere, remote sensing using atmospheric radiation; solar physics, infrared astronomy, infrared signature analysis; effects of solar activity, magnetic storms and nuclear explosions on the earth's atmosphere, ionosphere and magnetosphere; effects of electromagnetic and particulate radiations on space systems; space instrumentation; propellant chemistry, chemical dynamics, environmental chemistry, trace detection; atmospheric chemical reactions, atmospheric optics, light scattering, state-specific chemical reactions and radiative signatures of missile plumes, and sensor out-of-field-of-view rejection.